Title

Analytical approximation of transit time scattering due to magnetosonic waves

Permalink

https://escholarship.org/uc/item/0cz9w2bk

Journal

Geophysical Research Letters, 42(5)

ISSN

0094-8276

Authors

Bortnik, J
Thorne, RM
Ni, B
et al.

Publication Date

2015-03-16

DOI

10.1002/2014gl062710

Peer reviewed

Analytical approximation of transit time scattering due to magnetosonic waves

J. Bortnik[1], R. M. Thorne[1], B. Ni[2], and J. Li[3]

[1]Department of Atmospheric and Oceanic Sciences, University of California, Los Angeles, California, USA, [2]Department of Space Physics, School of Electronic Information, Wuhan University, Wuhan, China, [3]Institute of Space Physics and Applied Technology, Peking University, Beijing, China

Abstract Recent test particle simulations have shown that energetic electrons traveling through fast magnetosonic (MS) wave packets can experience an effect which is specifically associated with the tight equatorial confinement of these waves, known as transit time scattering. However, such test particle simulations can be computationally cumbersome and offer limited insight into the dominant physical processes controlling the wave-particle interactions, that is, in determining the effects of the various wave parameters and equatorial confinement on the particle scattering. In this paper, we show that such nonresonant effects can be effectively captured with a straightforward analytical treatment that is made possible with a set of reasonable, simplifying assumptions. It is shown that the effect of the wave confinement, which is not captured by the standard quasi-linear theory approach, acts in such a way as to broaden the range of particle energies and pitch angles that can effectively resonate with the wave. The resulting diffusion coefficients can be readily incorporated into global diffusion models in order to test the effects of transit time scattering on the dynamical evolution of radiation belt fluxes.

1. Introduction

Fast magnetosonic (MS) waves are a class of right-hand elliptically polarized, electromagnetic emissions that are found in the Earth's inner magnetosphere at L shells that straddle the plasmapause, $L \sim 2$–8 [*Gurnett*, 1976; *Perraut et al.*, 1982; *Laakso et al.*, 1990] and magnetic local time regions that favor the postnoon or dusk sectors [*Green et al.*, 2005; *Pokhotelov et al.*, 2008]. Typical observations show that MS waves occur as a series of narrow tones, spaced at multiples of the proton gyrofrequency (f_{ci}), in the range between f_{ci} and the lower hybrid resonance frequency (f_{LHR}), that are spatially localized near the geomagnetic equator within ~ 2–$3°$ [*Russell et al.*, 1970; *Santolik et al.*, 2002; *Nemec et al.*, 2005, 2006] (although larger spreads have occasionally been reported [*Tsurutani et al.*, 2014]) and propagate at angles that are nearly perpendicular to the background magnetic field which requires the wave magnetic field to be nearly parallel to the background field. MS waves are believed to derive their energy from unstable "ring" distributions in the ion population [e.g., *Gurnett*, 1976; *Perraut et al.*, 1982; *Boardsen et al.*, 1992; *Horne et al.*, 2000; *Meredith et al.*, 2008; *Xiao et al.*, 2013; *Ma et al.*, 2014], which form mostly on the dayside as a result of the overlap of the westward drifting energetic ions (due to gradient curvature drift) and eastward drifting cold ions (due to the corotation electric field), with a null near ~ 10 keV [e.g., *Chen et al.*, 2010].

MS waves have become the focus of renewed attention, following a study by *Horne et al.* [2007] that demonstrated the potential of these waves to accelerate radiation belt electrons to relativistic energies on timescales that are comparable to other leading mechanisms, i.e., ~ 1–2 days. However, due to the combination of high obliquity and tight spatial confinement of the MS waves, it was not clear that the quasi-linear diffusion theory employed by *Horne et al.* in their analysis was the most appropriate approach. In particular, *Bortnik and Thorne* [2010] showed that when a test particle simulation was performed, the energy range of resonant particles was significantly widened, and additional nulls appeared in the scattering map of electrons, due to an effect known as "transit time scattering" (analogous to an effect employed in an early method used to heat ions in magnetically confined plasmas [e.g., *Berger et al.*, 1958; *Stix*, 1992]). A drawback of test particle simulations is the long computation time required to produce a map of diffusion coefficients, and the relatively poor insight into the dominant physical processes controlling the particle scattering, that is, what effects do the various wave parameters (for example, the wave intensity, obliquity, and equatorial confinement) play in the pitch angle and energy scattering. Furthermore, since transit time

scattering was shown to be linear (but nonresonant), it is not clear that a full test particle simulation run is always necessary to obtain the relevant scattering properties.

In the present paper, we show that by using a few reasonable approximations, the equations describing the test particle motion through the MS wavefield become readily integrable and result in equations that smoothly capture the transition from resonant to nonresonant scattering and elucidate the dominant processes involved. In section 2 we present the derivation of the equations and discuss the results in section 3.

2. Analytical Approximation

As a starting point, we use the set of equations that describes the motion of a test particle in a static magnetic field $\left(\mathbf{B}_0 = B_0\hat{\mathbf{z}}\right)$, with a superimposed whistler mode wavefield having a wave number k, a wave normal angle ψ, and wave components $E_x^w, E_y^w, E_z^w, B_x^w, B_y^w$, and B_z^w. The equations are gyroaveraged and decomposed into a sum of harmonic resonances m:

$$\frac{dp_\parallel}{dt} = \omega_{\tau m}^2 m_e k_\parallel^{-1} \sin\eta - \frac{1}{m_e\gamma}\frac{p_\perp^2}{2\omega_{ce}}\frac{\partial\omega_{ce}}{\partial z}$$

$$\frac{dp_\perp}{dt} = -(-1)^{m-1}\left[\omega_1\left(\frac{p_\parallel}{\gamma} + m_e R_1\right)J_{m-1}(\beta) - \ldots \right. \tag{1}$$

$$\left. \omega_2\left(\frac{p_\parallel}{\gamma} - m_e R_2\right)J_{m+1}(\beta)\right]\sin\eta + \ldots$$

$$\frac{1}{m_e\gamma}\frac{p_\parallel p_\perp}{2\omega_{ce}}\frac{\partial\omega_{ce}}{\partial z} \tag{2}$$

$$\frac{d\eta}{dt} = \frac{m\omega_{ce}}{\gamma} - \omega - k_\parallel\frac{p_\parallel}{m_e\gamma} \tag{3}$$

where η is defined as the angle between B_R^w, $v_\perp$, ω is the whistler wave radial frequency, and $\omega_{ce} = -q_e B_0/m_e = eB_0/m_e$ is the electron gyrofrequency, where q_e and m_e are the electron charge and mass, respectively. J_i are Bessel functions of the first kind, order i, whose argument is proportional to the particle gyroradius in terms of perpendicular wavelengths and represents the asymmetry of the wavefield as experienced by the gyrating particle. The supporting equations are

$$\beta = \frac{k_\perp p_\perp}{m_e\omega_{ce}} \tag{4}$$

$$k_\parallel = k\cos\psi = (\omega\mu/c)\cos\psi; \quad k_\perp = k\sin\psi \tag{5}$$

$$\omega_{\tau m}^2 = (-1)^{m-1}\omega_{\tau 0}^2\left[J_{m-1}(\beta) - \alpha_1 J_{m+1}(\beta) + \gamma\alpha_2 J_m(\beta)\right] \tag{6}$$

$$\omega_{\tau 0}^2 = \frac{\omega_1 k_\parallel p_\perp}{\gamma m_e} \tag{7}$$

$$\omega_1 = \frac{e}{2m_e}\left(B_x^w + B_y^w\right); \quad \omega_2 = \frac{e}{2m_e}\left(B_x^w - B_y^w\right) \tag{8}$$

$$\alpha_1 = \frac{\omega_2}{\omega_1}; \quad \alpha_2 = \frac{eE_z^w}{\omega_1 p_\perp} \tag{9}$$

$$R_1 = \frac{E_x^w + E_y^w}{B_x^w + B_y^w}; \quad R_2 = \frac{E_x^w - E_y^w}{B_x^w - B_y^w} \tag{10}$$

where μ is the refractive index and ω_{r0} is the trapping frequency. The set of equations is closed by relating the wave components to a single reference component through the usual *Stix* [1992] relations. The nonlinear phase term in (3) is neglected as in previous studies, since it is generally a small correction and potentially only impacts particles at very low pitch angles [e.g., *Tao and Bortnik*, 2010].

We note explicitly that compared to the set of equations given in *Bortnik and Thorne* [2010], equation (2) differs by the inclusion of an additional factor $(-1)^{m-1}$ which causes a sign difference for the Landau ($m = 0$) and all even numbered harmonic resonances. The source of this discrepancy is shown and discussed in detail by *Li et al.* [2014].

Although the set of equations (1)–(3) may appear somewhat complicated at first glance, it is reduced fairly quickly by taking some straightforward assumptions. As in previous work [*Horne et al.*, 2007; *Bortnik and Thorne*, 2010] we consider only the $m = 0$ resonance, since resonant energies for $|m| \geq 1$ are in excess of 10 MeV and hence beyond our energy range of interest. Equation (3) can then be rewritten as

$$\frac{d\eta}{dt} = -\omega - k_{\parallel} v_{\parallel} \tag{11}$$

Furthermore, since MS waves are confined to near-equatorial regions, we do not need to use the full dipolar description of the background magnetic field but can expand the field near the equator using a Taylor series and retain only the second-order term, as was done in previous work [e.g., *Helliwell*, 1967, equation (8)], giving

$$B = B_0 \left(1 + \frac{4.5 z^2}{L^2 R_e^2} \right) = B_0 \left(1 + g z^2 \right) \tag{12}$$

where the substitution $g = 4.5 / \left(L^2 R_e^2 \right)$ has been made above. Through conservation of the first adiabatic invariant (i.e., $p_{\perp}^2 / B = p_{\perp 0}^2 / B_0$), we obtain the first-order variation of the particle's velocity components near the equator, substitute into (11) and rewrite the ordinary differential equation in terms of distance along the field line, z, giving

$$\frac{d\eta}{dz} = -\frac{\omega}{v_{\parallel}} - k_{\parallel} \tag{13}$$

$$= -\frac{\omega}{v_{\parallel 0} \sqrt{1 - \left(v_{\perp 0}^2 / v_{\parallel 0}^2 \right) g z^2}} - k_{\parallel} \tag{14}$$

$$\sim -\frac{\omega}{v_{\parallel 0}} \left(1 + \frac{v_{\perp 0}^2}{2 v_{\parallel 0}^2} g z^2 \right) - k_{\parallel} \tag{15}$$

In order to keep (15) simple and the complete set of equations tractable, we shall neglect the adiabatic variation of the particle velocity, such that
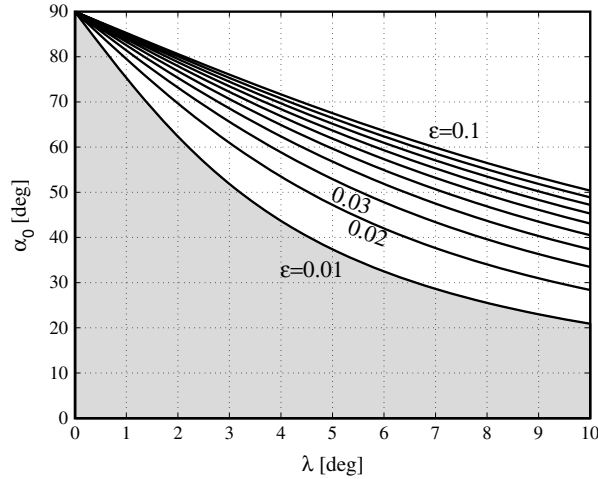
$$\frac{d\eta}{dz} = -\frac{\omega}{v_{\parallel 0}} - k_{\parallel} \tag{16}$$

which implies that

$$\epsilon = \frac{v_{\perp 0}^2}{2 v_{\parallel 0}^2} g z^2 \ll 1 \tag{17}$$

Near the equator, z can be expressed as a function of geomagnetic latitude λ (in degrees) for a dipolar magnetic field as

$$z = \lambda \frac{\pi}{180} L R_E \cos \lambda \sqrt{1 + 3 \sin^2 \lambda} \sim \lambda \frac{\pi}{180} L R_E \tag{18}$$

Figure 1. Validity condition for approximation of the dipolar magnetic field as a uniform field. The shaded region indicates where the approximation is accurate within 1%, as a function of equatorial pitch angle and geomagnetic latitude.

Substituting (18) into (17), using the relation $\tan \alpha_0 = v_{\perp 0}/v_{\parallel 0}$, where α_0 is the equatorial pitch angle and bearing in mind that $\epsilon \ll 1$, we obtain

$$g \left(\frac{\pi}{180} L R_E \right)^2 \lambda^2 \tan^2 \alpha_0 = 2\epsilon \quad (19)$$

$$\lambda \tan \alpha_0 = \sqrt{\frac{2\epsilon}{4.5}} \frac{180}{\pi} \sim 38 \sqrt{\epsilon} \quad (20)$$

The condition for validity (20) is plotted in Figure 1 and shows the relation between the maximum latitude λ within which our approximation holds and the maximum equatorial pitch angle of the interacting particle α_0, for 10 values of ϵ ranging from $\epsilon = 0.01$ (bottom curve) to $\epsilon = 0.1$ (top curve). Since the bulk of the magnetosonic wave power is primarily confined to $\lambda \sim 2°$–$3°$ of the equator, the pitch angle range where our approximation is valid extends from $\alpha_0 = 0°$ to approximately $\alpha_0 \sim 70°$–$80°$, which is quite adequate for our purposes.

We now integrate (16) once, to obtain

$$\eta = -\left(\frac{\omega}{v_{\parallel 0}} + k_{\parallel} \right) z + \eta_0 \quad (21)$$

where η_0 is a constant of integration and can be interpreted as the phase angle at $z = 0$.

Having performed the first integration of the phase, we now return to the variation of the particle's motion, namely, (1) and (2). Since the integration is assumed to be symmetrical about the geomagnetic equator, and the scattering is "small," the last term on the right-hand side of (1) and (2) describing the adiabatic variation of the particle's motion can be neglected to first order. We further assume that the leading multipliers of both equations do not vary significantly near the equator (as above), except for a variation in the wave amplitude of the form

$$B^w = B_0^w \exp\left(-\lambda^2 / \lambda_w^2 \right) \quad (22)$$

where B_0^w is the equatorial value of the MS wave's magnetic field and λ_w specifies its latitudinal confinement. This envelope of the wave intensity models the confinement of the wave to near-equatorial regions, as was done previously [*Bortnik and Thorne*, 2010]. The resulting equations both have a similar form and can be expressed as

$$\frac{dp_j}{dz} = \frac{A_j}{v_{\parallel 0}} \exp\left(-z^2 / z_w^2 \right) \sin(Bz + C) \quad (23)$$

where the differential equations have been rewritten as a function of z, which is related to λ as in (18) and the subscript j denotes either the parallel or perpendicular components of the particle motion, such that

$$A_{\parallel} = \frac{\omega_{\tau m}^2 m_e}{k_{\parallel 0}} \quad (24)$$

$$A_{\perp} = \left[\omega_1 \left(\frac{p_{\parallel}}{\gamma} + m_e R_1 \right) J_{-1}(\beta) - \ldots \right.$$
$$\left. \omega_2 \left(\frac{p_{\parallel}}{\gamma} - m_e R_2 \right) J_{+1}(\beta) \right] \quad (25)$$

and the $m = 0$ resonance has been explicitly assumed, as before. From (21), the values of B and C are

$$B = -\left(\frac{\omega}{v_{||0}} + k_{||}\right) \tag{26}$$

$$C = \eta_0 \tag{27}$$

Equations of the form (23) have an exact integral solution given by

$$\int \frac{A_j}{v_{||0}} \exp\left(-\frac{z^2}{z_w^2}\right) \sin(Bz + C) \mathrm{d}z = \frac{\sqrt{\pi}}{2} \frac{A_j}{v_{||0}} z_w \sin C \exp\left(-\frac{z_w^2 B^2}{4}\right) \Re\left[\mathrm{erf}\left(\frac{z}{z_w} + \frac{iz_w B}{2}\right)\right] \tag{28}$$

which can then be evaluated between the limits $\pm z_1$ as a definite integral. Furthermore, if it is assumed that the limits of integration are much larger than the extent of the wave, i.e., $z_1/z_w > 4$ (or so), the error function tends to unity and the definite integral takes on the relatively simple form:

$$\Delta p_j = \int_{-z_1}^{z_1} \frac{A_j}{v_{||0}} \exp\left(-\frac{z^2}{z_w^2}\right) \sin(Bz + C)\, \mathrm{d}z = \sqrt{\pi} \frac{A_j}{v_{||0}} z_w \sin C \exp\left(-\frac{z_w^2 B^2}{4}\right) \tag{29}$$

Similar analytical expressions can be derived for the variation in the particle's pitch angle and energy. For instance, starting with the definition $\tan \alpha = p_\perp/p_{||}$ and taking the derivative yields

$$\frac{\mathrm{d}\alpha}{\mathrm{d}t} = \frac{\cos\alpha}{p}\frac{\mathrm{d}p_\perp}{\mathrm{d}t} - \frac{\sin\alpha}{p}\frac{\mathrm{d}p_{||}}{\mathrm{d}t} \tag{30}$$

which has the same form as equations (1)–(2) and can be reduced to the form of (29) by letting

$$A_j = A_\alpha = \frac{\cos\alpha_0}{p_0}A_\perp - \frac{\sin\alpha_0}{p_0}A_{||} \tag{31}$$

Similarly, the variation in particle energy can be related to the variation in the particle momentum components in a straightforward way. The rate of change of particle energy is

$$\frac{\mathrm{d}E}{\mathrm{d}t} = m_e c^2 \frac{\mathrm{d}\gamma}{\mathrm{d}t} = \frac{m_e c^2}{2\gamma}\frac{\mathrm{d}\gamma^2}{\mathrm{d}t} = \frac{m_e c^2}{2\gamma}\frac{\mathrm{d}}{\mathrm{d}t}\left(1 + \frac{p^2}{m_e^2 c^2}\right) \tag{32}$$

Writing $p^2 = p_\perp^2 + p_{||}^2$, (32) can be expressed in terms of (1)–(2) as

$$\frac{\mathrm{d}E}{\mathrm{d}t} = v_{||}\frac{\mathrm{d}p_{||}}{\mathrm{d}t} + v_\perp\frac{\mathrm{d}p_\perp}{\mathrm{d}t} \tag{33}$$

which reduces to the form of (29) by letting

$$A_j = A_E = v_{||0}(A_{||} + \tan\alpha_0 A_\perp) \tag{34}$$

Equations (31) and (34) have been evaluated together with (29) and compared to the integration of the full differential equations, showing that the agreement is excellent (Figure 2).

The equations for the diffusion coefficients due to equatorially confined MS waves can be related to the variation in the particle's properties in a simple way:

$$D_{ij} = \frac{\langle \Delta p_i \Delta p_j \rangle}{2\tau} \tag{35}$$

where i, j denote any two properties of the particle, such as energy and pitch angle described by (31) and (34). The timescale τ is the timescale over which the wave-particle interaction took place, and in our case
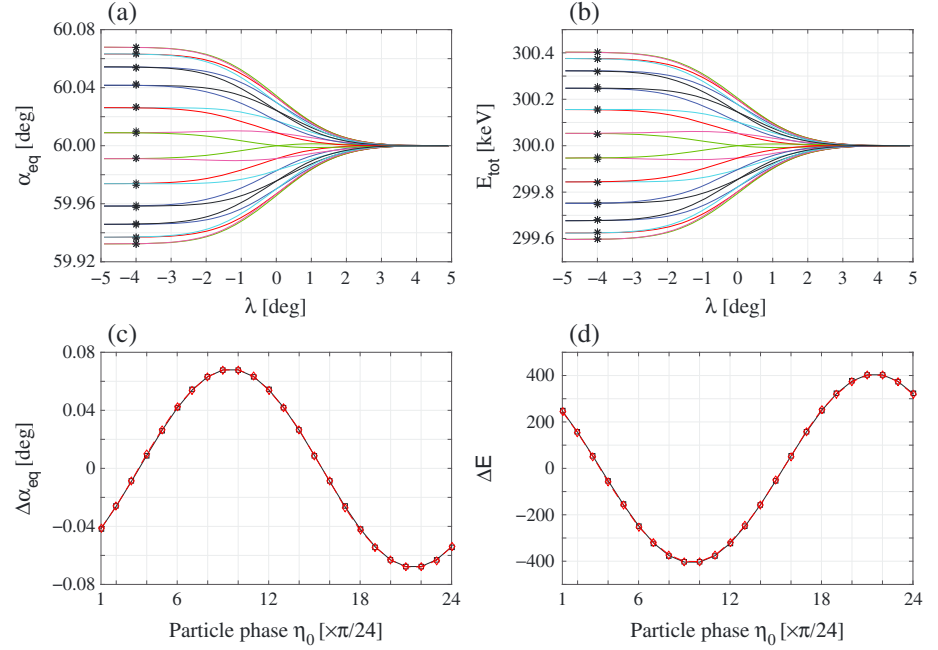
Figure 2. A comparison between analytically derived and numerically computed scattering in energy and pitch angle. (a and b) The latitude-dependent trajectories of 24 electrons, together with analytical estimates plotted as stars at $\lambda = -4°$. (c and d) The net scattering calculated numerically (black solid line) and analytically (red dashed line).

$\tau = 0.5\tau_b$ since (29) describes only a single transit across the equator, i.e., a half-bounce period. The angled brackets "<>" indicate an averaging over gyrophase, and in the case of (29) is simplified by the relation:

$$\int_0^{2\pi} \sin^2(\eta_0)d\eta_0 = 1/2 \tag{36}$$

Inserting (36), (31), and (34) into (35) gives the energy, pitch angle, and cross diffusion coefficients

$$D_{EE} = \frac{\pi A_E^2}{2\tau_b E_0^2} \left(\frac{z_w}{v_{||0}}\right)^2 \exp\left[-\left(\frac{z_w}{v_{||0}}\right)^2 \frac{(\omega + k_{||}v_{||0})^2}{2}\right] \tag{37}$$

$$D_{\alpha\alpha} = \frac{\pi A_\alpha^2}{2\tau_b} \left(\frac{z_w}{v_{||0}}\right)^2 \exp\left[-\left(\frac{z_w}{v_{||0}}\right)^2 \frac{(\omega + k_{||}v_{||0})^2}{2}\right] \tag{38}$$

and

$$D_{\alpha E} = \frac{\pi A_\alpha A_E}{2\tau_b E_0} \left(\frac{z_w}{v_{||0}}\right)^2 \exp\left[-\left(\frac{z_w}{v_{||0}}\right)^2 \frac{(\omega + k_{||}v_{||0})^2}{2}\right] \tag{39}$$

3. Discussion

The analytical expressions in (37) and (39) have a simple form and show that the term $(z_w/v_{||0})^2$ is introduced into the diffusion equation due to the spatial confinement of MS wave described in (22). This term can be thought of as the timescale required for the particle to transit through the wave packet, $\tau_{tr} = z_w/v_{||0}$, and has the effect of scaling both the magnitude of the diffusion coefficients, and the phase term, $\phi = \omega + k_{||}v_{||0}$ (we remind the reader that the senses of k and $v_{||0}$ are defined positive in opposite directions in accordance with *Bell* [1984] and for historical reasons [e.g., *Inan et al.*, 1978; *Helliwell*, 1967]).

When the particle propagating through the MS wave packet is in Landau resonance, $\phi = 0$, the exponential term becomes unity, reducing to the ordinary quasi-linear diffusion coefficient which is then simply scaled by the extent of the wave packet. However, when particles are not strictly in resonance, $\phi \neq 0$ and the
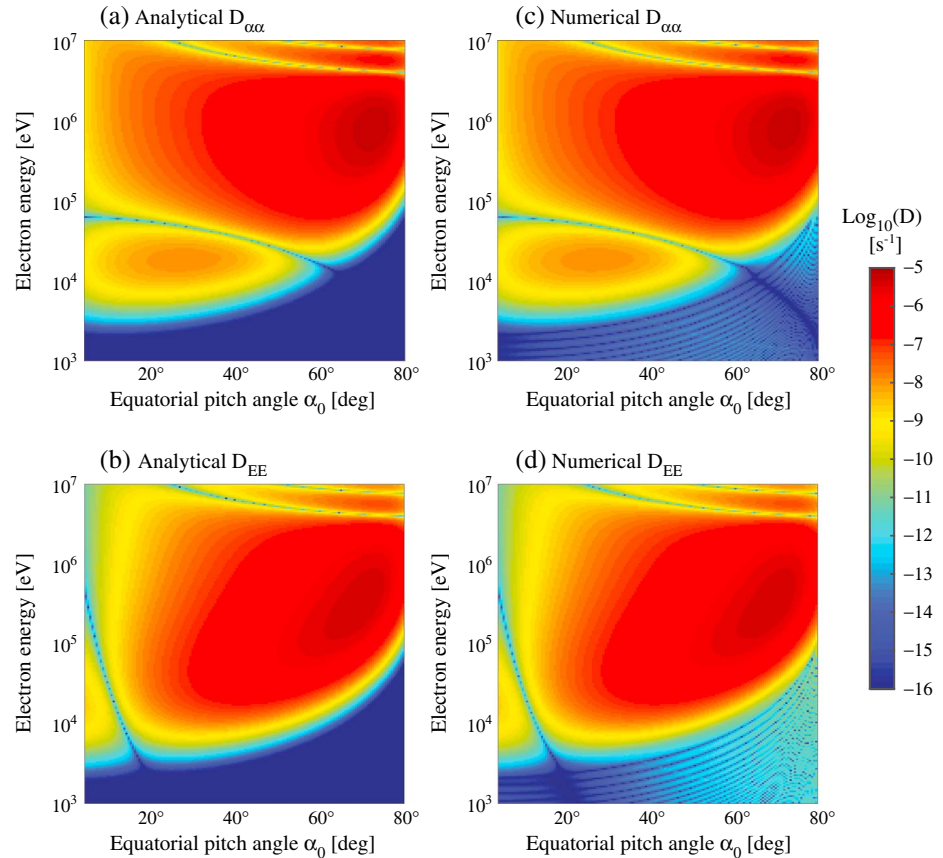
Figure 3. A comparison of (a and b)analytically and (c and d) numerically computed diffusion coefficients, $D_{\alpha\alpha}$ (Figures 3 and 3c) and D_{EE} (Figures 3b and 3d). The color axis is in units of s^{-1}.

exponential term can become ~ 0, thus severely reducing the magnitude of the diffusion coefficient. In this case, having a narrowly confined wave packet, i.e., $\tau_{tr} \ll 1$ scales the phase term ϕ such that the overall argument of the exponential $\tau_{tr}^2 \phi^2/2 \ll 1$, and the exponential term can still take on values ~ 1. This effect of the wave confinement is not captured by the standard quasi-linear theory approach and acts in such a way as to broaden the range of particle energies and pitch angles that can effectively "resonate" with the wave.

Figure 3 shows an evaluation of (37) and (39) for the set of parameters described by *Bortnik and Thorne* [2010] section 2.2 and is compared to a full test particle simulation in Figures 3a and 3b and Figures 3c and 3d, respectively. The figure serves to demonstrate that the agreement between our analytical formulas and the full simulation is excellent, and the simplifying assumptions we have employed did not degrade the results. The difference in computation time, however, is dramatic, the analytical evaluation taking approximately 4 orders of magnitude faster to compute than the full test particle simulation (a few seconds compared to about 10 h on the same computer). This evaluation was performed over a similar energy and pitch angle range as the full test particle simulation in Figure 4 of *Bortnik and Thorne* [2010] and shows excellent agreement when the additional $(-1)^{m-1}$ term is included in the latter. The figure also shows similar null patterns in the figures, although the low-amplitude harmonic ripples are typically not captured.

Our analysis shows that the nonresonant effects introduced by the confinement of the wave packet can be effectively captured with a straightforward analytical treatment that is made possible with a set of reasonable, simplifying assumptions. These expressions can be readily incorporated into global diffusion models in order to test the effect of transit time scattering on the dynamical evolution of radiation belt fluxes.

References

Bell, T. F. (1984), The nonlinear gyroresonance interaction between energetic electrons and coherent VLF waves propagating at an arbitrary angle with respect to the Earth's magnetic field, *J. Geophys. Res.*, *89*(A2), 905–918.

Berger, J. M., W. A. Newcomb, J. M. Dawson, E. A. Frieman, R. M. Kulsrud, and A. Lenard (1958), Heating of a confined plasma by oscillating electromagnetic fields, *Phys. fluids*, *1*(4), 301–307.

Boardsen, S. A., D. L. Gallagher, D. A. Gurnett, W. K. Peterson, and J. L. Green (1992), Funnel-shaped low-frequency equatorial waves, *J. Geophys. Res.*, *97*, 14,967–14,976.

Bortnik, J., and R. N. Thorne (2010), Transit time scattering of energetic electrons due to equatorially confined magnetosonic waves, *J. Geophys. Res.*, *115*, A07213, doi:10.1029/2010JA015283.

Chen, L., R. M. Thorne, V. K. Jordanova, and R. B. Horne (2010), Global simulation of magnetosonic wave instability in the storm time magnetosphere, *J. Geophys. Res.*, *115*, A11222, doi:10.1029/2010JA015707.

Green, J. L., S. Boardsen, L. Garcia, W. W. L. Taylor, S. F. Fung, and B. W. Reinisch (2005), On the origin of whistler mode radiation in the plasmasphere, *J. Geophys. Res.*, *110*, A03201, doi:10.1029/2004JA010495.

Gurnett, D. A. (1976), Plasma wave interactions with energetic ions near the magnetic equator, *J. Geophys. Res.*, *81*, 2765–2770.

Helliwell, R. A. (1967), A theory of discrete VLF emissions from the magnetosphere, *J. Geophys. Res.*, *72*(19), 4773–4790.

Horne, R. B., G. V. Wheeler, and H. S. C. K. Alleyne (2000), Proton and electron heating by radially propagating fast magnetosonic waves, *J. Geophys. Res.*, *105*, 27,597–27,610.

Horne, R. B., R. M. Thorne, S. A. Glauert, N. P. Meredith, D. Pokhotelov, and O. Santolik (2007), Electron acceleration in the Van Allen radiation belts by fast magnetosonic waves, *Geophys. Res. Lett.*, *34*, L17107, doi:10.1029/2007GL030267.

Inan, U. S., T. F. Bell, and R. A. Helliwell (1978), Nonlinear pitch angle scattering of energetic electrons by coherent VLF waves in the magnetosphere, *J. Geophys. Res.*, *83*(A7), 3235–3253.

Laakso, H., H. Junginger, A. Roux, R. Schmidt, and C. de Villedary (1990), Magnetosonic waves above fcH+ at geostationary orbit: GEOS 2 results, *J. Geophys. Res.*, *95*, 10,609–10,621.

Li, J., et al. (2014), Interactions between magnetosonic waves and radiation belt electrons: Comparisons of quasi-linear calculations with test particle simulations, *Geophys. Res. Lett.*, *41*, 4828–4834, doi:10.1002/2014GL060461.

Ma, Q., W. Li, L. Chen, R. M. Thorne, and V. Angelopoulos (2014), Magnetosonic wave excitation by ion ring distributions in the Earth's inner magnetosphere, *J. Geophys. Res. Space Physics*, *119*, 844–852, doi:10.1002/2013JA019591.

Meredith, N. P., R. B. Horne, and R. R. Anderson (2008), Survey of magnetosonic waves and proton ring distributions in the Earth's inner magnetosphere, *J. Geophys. Res.*, *113*, A06213, doi:10.1029/2007JA012975.

Nemec, F., O. Santolik, K. Gereova, E. Macusova, Y. de Conchy, and N. Cornilleau-Wehrlin (2005), Initial results of a survey of equatorial noise emissions observed by the Cluster spacecraft, *Planet. Space Sci.*, *53*, 291–298.

Nemec, F., O. Santolik, K. Gereova, E. Macusova, H. Laakso, Y. de Conchy, M. Maksimovic, and N. Cornilleau-Wehrlin (2006), Equatorial noise: Statistical study of its localization and the derived number density, *Adv. Space Res.*, *37*, 610–616.

Perraut, S., A Roux, P. Robert, R. Gendrin, J. A. Sauvaud, J. M. Bosqued, G. Kremser, and A. Korth (1982), A systematic study of ULF waves above FH+ from GEOS 1 and 2 measurements and their relationships with proton ring distributions, *J. Geophys. Res.*, *87*, 6219–6236.

Pokhotelov, D., F. Lefeuvre, R. B. Horne, and N. Cornilleau-Wehrlin (2008), Survey of ELF-VLF plasma waves in the outer radiation belt observed by Cluster STAFF-SA experiment, *Ann. Geophys.*, *26*, 3269–3277.

Russell, C. T., R. E. Holzer, and E. J. Smith (1970), OGO 3 observations of ELF noise in the magnetosphere. The nature of equatorial noise, *J. Geophys. Res.*, *75*, 755–768.

Santolik, O., J. S. Pickett, D. A. Gurnett, M. Maksimovic, and N. Cornilleau-Wehrlin (2002), Spatiotemporal variability and propagation of equatorial noise observed by Cluster, *J. Geophys. Res.*, *107*(A12), 1495, doi:10.1029/2001JA009159.

Stix, T. H. (1992), *Waves in Plasmas*, Springer, New York.

Tao, X., and J. Bortnik (2010), Nonlinear interactions between relativistic radiation belt electrons and oblique whistler mode waves, *Nonlinear Processes Geophys.*, *17*, 599–604, doi:10.5194/npg-17-599-2010.

Tsurutani, B. T., B. J. Falkowski, J. S. Pickett, O. P. Verkhoglyadova, O. Santolik, and G. S. Lakhina (2014), Extremely intense ELF magnetosonic waves: A survey of polar observations, *J. Geophys. Res. Space Physics*, *119*, 964–977, doi:10.1002/2013JA019284.

Xiao, F., Q. Zhou, Z. He, C. Yang, Y. He, and L. Tang (2013), Magnetosonic wave instability by proton ring distributions: Simultaneous data and modeling, *J. Geophys. Res. Space Physics*, *118*, 4053–4058, doi:10.1002/jgra.50401.